UNDER PEER REVIEW

Original Research Article

Dynamics and analysis of chronic brucellosis in sheep

Abstract

In this work, we proposed and studied a new fractional-order model for the transmission dynamics of *brucellosis* with a special focus on the sheep-to-sheep transmission. Two control strategies namely; culling and vaccination rate are incorporated in the model. We computed the basic reproduction number $\mathcal{R}_0$ and we studied the global stability of disease-free and endemic equilibrium point in terms of basic reproduction number $\mathcal{R}_0$. We found that both the disease-free and endemic equilibrium points are globally stable whenever $\mathcal{R}_0 < 1$ and $\mathcal{R}_0 > 1$ respectively. In numerical simulations, we performed the sensitivity analysis of the model and expressed the relationship between model parameters and $\mathcal{R}_0$. We noted that, increase on the magnitude of model parameters with negative correlation coefficients would significantly reduce the spread of Brucellosis disease in the population. Moreover, model validation and parameter estimation for fractional-order and classical integer-order derivatives was carried out using real *brucellosis* data for Egypt, 1999-2011. Overall, we noted that fractional-order model gave better prediction of *brucellosis* compared to classical integer-order model. Furthermore, we investigated the role of memory effects on the transmission of *brucellosis* in the population. We observe that, the memory effects have influence on the transmission of *brucellosis* in the community. In addition, we noted that the aforementioned control strategies have the potential to reduce the transmission

of *brucellosis* in the population. In particular, we observed that whenever the culling and vaccination rate is greater than 40% and 50% respectively, the disease dies out in the population.

Keywords: Brucellosis, Fractional-order model, Global stability, Sensitivity analysis, parameter estimation.

1 Introduction

Globally, human *brucellosis* remains an important and widespread infection [1]. *Brucella melitensis* is responsible for the vast majority of human cases [2]. Sheep and goats represent the natural hosts of *B. melitensis* [3, 4]. Domesticated species such as cattle, sheep, horse and goats are regarded as the main source of human *brucellosis* [5], in which transmission may occur directly or through the consumption of unpasteurised dairy products [6]. The infection is transmitted to humans mainly by direct contact with animals or by consumption of milk products [7]. Although the disease is well contained in Australia and the UK, the annual global incidence of *brucellosis* is estimated above 500 000 [8, 9]. *Brucellosis* is endemic in Mediterranean areas, the south and the center of America, Africa, Asia, Arab peninsula, Indian subcontinent and the Middle East [5]. In animals, *brucellosis* is transmitted by direct contact transmission through the *brucella* carriers or indirect contact transmission when animals ingest contaminated forages or the excrement containing large quantities of bacteria, generally discharged by infected animals [6].

Since human-to-human transmission of the disease is rare the ultimate management of human brucellosis can be achieved through effective control of brucellosis in animal population. In addition the number one Sustainable Development Goal concerns ending poverty. Household income is identified as the major way by which extreme poverty can be reduced in developing countries. As a result, stake-holders and policy makers have turned their focus on livestock production as a means of raising income and improving the livelihood of rural dwellers. The livestock industry does not only supply manure for crop and vegetable growers but it also ensures the sustainability of food and nutrients and financial security, all of which contribute to raise the standard of living, particularly in rural areas.

Mathematical models have proved to be essential guiding tools for epidemiologists, biologists as well as policy makers. Recently, modelling the transmission dynamics of *brucellosis*, is one of the most common global zoonoses [10], has been an interesting topic for a number of researchers (see, for example [6, 11, 12, 13, 14, 15, 16, 17, 18, 19]). It is undeniable that these studies and several other have produced several useful results and significantly improved the existing knowledge on *brucellosis* dynamics. Understanding the role of memory effects on short and long-term dynamics of infectious diseases is one of the emerging areas in the biological research. Thus, in this study a mathematical model for *brucellosis* based on Fractional Calculus (FC) is proposed and analyzed. Although this study is not the first to incorporate FC in studying *brucellosis* transmission (see, for example [20]) the proposed model is unique from those in literature.

Although the fractional derivative has several definitions such as those derived from Riemann-Liouville, Caputo, liouville, Weyl, Riesz, Grunwald-Litnikov, Marchaud and Hifler, Caputo-Fabrizio-Caputo, Atanga-Baleanu, Atanga-beta derivative, $\mathbb{M}$-fractional derivative, Atangana-Koca, conformable derivative, Atanga-Gomez, Variable-order and fractal-fractional idea [21, 22], the model proposed in this study will be based on the Caputo derivative. The rationale of choosing the Caputo derivative is that the Caputo derivative for a given function which is constant is zero. Thus, the Caputo operator computes an ordinary differential equation, followed by a fractional integral to obtain the desired order of fractional derivative [20, 23, 24, 25]. Most importantly, the Caputo fractional derivative allows the use of local initial conditions to be included in the derivation of the model [20, 23, 24, 25].

To the best of our knowledge, none of the models proposed as of to date has incorporated the aspect of chronic animals. According to Evermann and Eriks [26], *brucellosis* ecology can be segmented as infection rate, attack rate (progression to clinical disease) and mortality/morbidity (chronic carrier state). Most common clinical signs of *brucellosis* infection in sheep are abortions, stillbirths and the birth of weak offspring. A given number of animals born from *brucella* infected females may be latent carriers (approximately 5%) and can only be identified by immunological tests after their first or second pregnancy [27, 28]. However, according to some researchers animals infected with *brucellosis* generally abort only once [29], and clearly if the animal is not detected at this stage it will become chronic. Undoubtedly, effective

management of *brucellosis* can be attained if emphasis is placed on multidisciplinary research aimed at addressing the underlying relationship between the disease ecology and prevalence.

The remainder of this paper is organized as follows. In Section 2, we present preliminaries on the Caputo fractional calculus. Followed by the proposed model and analytical results in Section 3. In Section 4, numerical simulations are done in order to verify theoretical results presented in the study. Finally, we conclude the paper with a concluding remark in Section 5.

2 Preliminaries on the Caputo fractional calculus

We begin by introducing the definition of Caputo fractional derivative and state related theorems (see, [30]) that we will utilise to derive important results in this work.

Definition 1. *Suppose that* $\alpha > 0, t > b, \alpha, b, t \in \mathbb{R}$. *The Caputo fractional derivative is given by*

$$ {}_b^c D_t^\alpha f(t) \frac{1}{\Gamma(n-\alpha)} \int_b^t \frac{f^n(\xi)}{(t-\xi)^{\alpha+1-n}} d\xi, \quad n-1 < \alpha, n \in \mathbb{N}. \tag{1} $$

Definition 2. *(Linearity property [30]). Let* $f(t), g(t) : [0, b] \to \mathbb{R}$ *be such that* ${}_b^c D_t^\alpha f(t)$ *and* ${}_b^c D_t^\alpha g(t)$ *exist almost everywhere and let* $c_1, c_2 \in \mathbb{R}$. *Then,* ${}_b^c D_t^\alpha (c_1 f(t)) +_b^c D_t^\alpha (c_2 g(t))$ *exists everywhere, and*

$$ {}_b^c D_t^\alpha (c_1 f(t) + c_2 g(t)) = c_1 \, {}_b^c D_t^\alpha f(t) + c_2 \, {}_b^c D_t^\alpha g(t). \tag{2} $$

Definition 3. *(Caputo derivative of a constant [24]). The fractional derivative for a constant function* $f(t) = a$ *is zero, that is,*

$$ {}_b^c D_t^\alpha a = 0. \tag{3} $$

Let us consider the following general type of fractional differential equations involving Caputo derivative:

$$ {}_b^c D_t^\alpha x(t) = f(t, x(t)), \qquad \alpha \in (0, 1), \tag{4} $$

with initial condition $x_0 = x(b)$.

Theorem 2.1. *(Uniform Asymptotic Stability [30, 31]). Let x^* be an equilibrium point for the non-autonomous fractional order system (4) and $\Omega \subset \mathbb{R}^n$ be a domain containing x^*. Let $L : [0, \infty) \times \Omega \to \mathbb{R}$ be a continuously differentiable function such that*

$$\mathcal{M}_1(x) \leq \mathcal{N}(t, x(t)) \leq \mathcal{M}_2(x)$$

and

$${}_0^c D_t^\alpha \mathcal{N}(t, x(t)) \leq \mathcal{M}_3(x),$$

for all $\alpha \in (0, 1)$ and all $x \in \Omega$, where $\mathcal{M}_1(x)$, $\mathcal{M}_2(x)$ and $\mathcal{M}_3(x)$ are continuous positive definite functions on Ω. Then the equilibrium point of system (4) is uniformly asymptotically stable.

3 Model Formulation and Analytical Results

We subdivide the total population of animals $N(t)$ at time t into compartments of: susceptible $S(t)$, vaccinated $H(t)$, exposed $E(t)$, clinically infected $I(t)$, and chronic carrier state $L(t)$. Thus, $N(t) = S(t) + H(t) + E(t) + I(t) + L(t)$: Susceptible animals are exposed to the disease through direct contact with exposed, clinically infected and chronic animals. Although, *brucellosis* can be transmitted indirectly (environmental transmission), prior studies [11, 12] suggest that form of transmission plays a relatively small role on the spread of *brucellosis*, and as such we have ignored this aspect in our study. The model flow chart and corresponding fractional-order equations for *brucellosis* dynamics are given below:

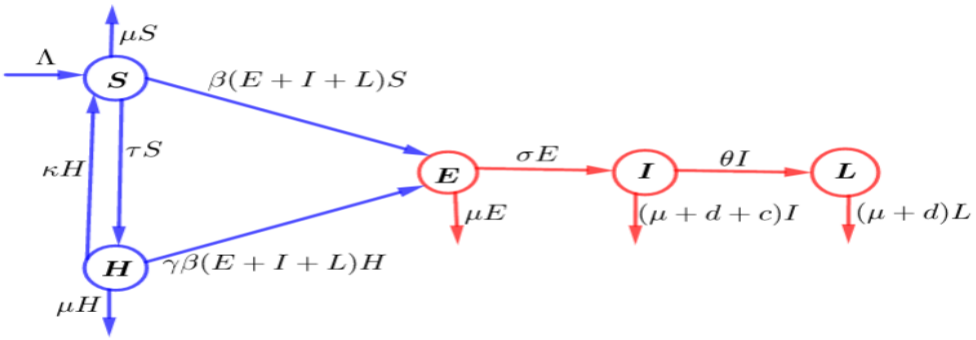

Figure 1: The model flow chart of *brucellosis* transmission

$$\left.\begin{aligned}
{}_b^cD_t^\alpha S(t) &= \Lambda^\alpha - \beta^\alpha(E(t)+I(t)+L(t))S(t) + \kappa^\alpha H(t) - (\mu^\alpha+\tau^\alpha)S(t),\\
{}_b^cD_t^\alpha H(t) &= \tau^\alpha S(t) - \gamma^\alpha\beta^\alpha(E(t)+I(t)+L)H(t) - (\kappa^\alpha+\mu^\alpha)H(t),\\
{}_b^cD_t^\alpha E(t) &= \beta^\alpha(E(t)+I(t)+L(t))(S(t)+\gamma^\alpha H(t)) - (\mu^\alpha+\sigma^\alpha)E(t),\\
{}_b^cD_t^\alpha I(t) &= \sigma^\alpha E(t) - (\mu^\alpha+\theta^\alpha+d^\alpha+c^\alpha)I(t),\\
{}_b^cD_t^\alpha L(t) &= \theta^\alpha I(t) - (\mu^\alpha+d^\alpha)L(t),
\end{aligned}\right\} \tag{5}$$

where ${}_b^cD_t^\alpha$ denotes the Caputo-fractional calculus and α with $0 < \alpha \leq 1$ is fractional order.

Where the death rate is denoted by μ, the parameter Λ is the recruitment rate, d is the disease-related death rate, τ is the vaccination rate, κ is the immunity waning rate, β is the disease direct transmission rate, γ is the modification factor, σ is the incubation rate, c is the culling rate of symptomatic infectious animals, and θ is the rate of progression to chronic state. All model parameter and variables are considered to be positive.

3.1 The Basic Reproduction Number and Existence of Equilibria

In this section, we study the basic reproduction number and the existence of a disease-free equilibrium and an endemic equilibrium of system (5). System (5) always has a disease-free equilibrium $\mathcal{E}^0 = (S^0, H^0, E^0, I^0, L^0) = (S^0, H^0, 0, 0, 0)$, with $S^0 = \frac{\Lambda^\alpha(\kappa^\alpha+\mu^\alpha)}{\mu^\alpha(\mu^\alpha+\kappa^\alpha+\tau^\alpha)}$, $H^0 = \frac{\Lambda^\alpha\tau^\alpha}{\mu^\alpha(\mu^\alpha+\kappa^\alpha+\tau^\alpha)}$, and $S^0+\gamma^\alpha H^0 = \frac{\Lambda^\alpha(\mu^\alpha+\kappa^\alpha+\gamma^\alpha\tau^\alpha)}{\mu^\alpha(\mu^\alpha+\kappa^\alpha+\tau^\alpha)}$. By means of the method of the next generation matrix (see, for example, van den Driessche and Watmough [32] , one obtains the basic reproduction number of system (5) as follows:

$$\begin{aligned}
\mathcal{R}_0 &= \mathcal{R}_E + \mathcal{R}_I + \mathcal{R}_L\\
&= \frac{\beta^\alpha(S^0+\gamma^\alpha H^0)}{(\mu^\alpha+\sigma^\alpha)} + \frac{\beta^\alpha\sigma^\alpha(S^0+\gamma^\alpha H^0)}{(\mu^\alpha+\sigma^\alpha)(\mu^\alpha+\theta^\alpha+d^\alpha+c^\alpha)}\\
&+ \frac{\beta^\alpha\sigma^\alpha\theta^\alpha(S^0+\gamma^\alpha H^0)}{(\mu^\alpha+\sigma^\alpha)(\mu^\alpha+\theta^\alpha+d^\alpha+c^\alpha)(\mu^\alpha+d^\alpha)}
\end{aligned} \tag{6}$$

$\mathcal{R}_0$ is the average number of secondary transmissions by a single infectious individual in a fully susceptible population,

where

- $\mathcal{R}_E = \frac{\beta^\alpha(S^0+\gamma^\alpha H^0)}{(\mu^\alpha+\sigma^\alpha)}$, accounts for the average number of new infections generated by exposed animals;

- $\mathcal{R}_I = \dfrac{\beta^\alpha \sigma^\alpha (S^0 + \gamma^\alpha H^0)}{(\mu^\alpha + \sigma^\alpha)(\mu^\alpha + \theta^\alpha + d^\alpha + c^\alpha)}$, gives the number of new infections generated by infectious animals; and;
- $\mathcal{R}_L = \dfrac{\beta^\alpha \sigma^\alpha \theta^\alpha (S^0 + \gamma^\alpha H^0)}{(\mu^\alpha + \sigma^\alpha)(\mu^\alpha + \theta^\alpha + d^\alpha + c^\alpha)(\mu^\alpha + d^\alpha)}$, measures the average number of secondary brucellosis infections generated by chronically infected animals.

In addition to the disease-free equilibrium $\mathcal{E}^0$, system (5) has a unique endemic equilibrium $\mathcal{E}^* = (S^*, H^*, E^*, I^*, L^*)$, where from the last two equations in (5) we have,

$$I^* = \frac{\sigma^\alpha E^*}{(\mu^\alpha + \theta^\alpha + d^\alpha + c^\alpha)}, L^* = \frac{\theta^\alpha \sigma^\alpha E^*}{(\mu^\alpha + \theta^\alpha + d^\alpha + c^\alpha)(\mu^\alpha + d^\alpha)}, \text{and} \quad (E^* + I^* + L^*) = ME^* \tag{7}$$

with

$$M = \frac{(\mu^\alpha + d^\alpha)(\mu^\alpha + \theta^\alpha + d^\alpha + c^\alpha) + \sigma^\alpha(\mu^\alpha + \theta^\alpha + d^\alpha)}{(\mu^\alpha + d^\alpha)(\mu^\alpha + \theta^\alpha + d^\alpha + c^\alpha)} \tag{8}$$

the first two equations in (5) lead to

$$S^* = \frac{\Lambda^\alpha(\mu^\alpha + \kappa^\alpha + \gamma^\alpha \beta^\alpha M E^*)}{(\mu^\alpha + \tau^\alpha + \beta^\alpha M E^*)(\mu^\alpha + \kappa^\alpha + \gamma^\alpha \beta^\alpha M E^*) - \kappa^\alpha \tau^\alpha}, \quad , \quad \text{and}$$

$$H^* = \frac{\Lambda^\alpha \tau^\alpha}{(\mu^\alpha + \tau^\alpha + \beta^\alpha M E^*)(\mu^\alpha + \kappa^\alpha + \gamma^\alpha \beta^\alpha M E^*) - \kappa^\alpha \tau^\alpha}, \tag{9}$$

for $E^* \neq 0$, substituting the third equation in (7) into the third equation in (5) yields,

$$(S^* + \gamma^\alpha H^*) = \frac{(\sigma^\alpha + \mu^\alpha)}{\beta^\alpha M}. \tag{10}$$

Substituting (9) into (10) gives:

$$F(E^*) = \frac{\Lambda^\alpha(\mu^\alpha + \kappa^\alpha + \gamma^\alpha \beta^\alpha M E^*) + \gamma^\alpha \Lambda^\alpha \tau^\alpha}{(\mu^\alpha + \tau^\alpha + \beta^\alpha M E^*)(\mu^\alpha + \kappa^\alpha + \gamma^\alpha \beta^\alpha M E^*) - \kappa^\alpha \tau^\alpha} - \frac{(\sigma^\alpha + \mu^\alpha)}{\beta^\alpha M}. \tag{11}$$

Direct calculation for $E^* \geq 0$ shows:

$${}_b^c D_t^\alpha F(E^*) = -\frac{\Lambda^\alpha M \beta^\alpha [(\gamma^\alpha \Lambda^\alpha \beta^\alpha E^*)^2 + 2(\gamma^\alpha \Lambda^\alpha \beta^\alpha E^*)(\mu^\alpha + \kappa^\alpha + \gamma^\alpha \tau^\alpha) + a]}{[(\mu^\alpha + \tau^\alpha + \beta^\alpha M E^*)(\mu^\alpha + \kappa^\alpha + \gamma^\alpha \beta^\alpha M E^*) - \kappa^\alpha \tau^\alpha]^2} < 0. \tag{12}$$

Where

$$a = (\mu^\alpha)^2 + 2\mu^\alpha \kappa^\alpha + (\kappa^\alpha)^2 + 2\gamma^\alpha \kappa^\alpha \tau^\alpha + 2\gamma^\alpha \mu^\alpha \tau^\alpha + (\gamma^\alpha \tau^\alpha)^2, \tag{13}$$

then the function $F(E^*)$ is monotonic decreasing for $E^* > 0$, then we can define the function

$$F(0) = \frac{\Lambda^\alpha(\mu^\alpha + \kappa^\alpha + \gamma^\alpha \tau^\alpha)}{\mu^\alpha(\mu^\alpha + \kappa^\alpha + \tau^\alpha)} - \frac{(\sigma^\alpha + \mu^\alpha)}{\beta^\alpha M} = \frac{(\sigma^\alpha + \mu^\alpha)}{\beta^\alpha M}(\mathcal{R}_0 - 1). \tag{14}$$

Therefore, by monotonicity of a function $F(E^*)$ there exists a unique positive root in the interval $(0, 1)$ when $\mathcal{R}_0 > 1$ and there is no positive root in the interval $(0, 1)$ when $\mathcal{R}_0 < 1$. Thus model (5) has a unique endemic equilibrium $\mathcal{E}^* = (S^*, H^*, E^*, I^*, L^*)$.

3.2 Global Stability

In this section, we are concerned with the global stability of the disease-free equilibrium $\mathcal{E}^0$ and the endemic equilibrium $\mathcal{E}^*$ of system (5).

Theorem 3.1. *If $\mathcal{R}_0 \leq 1$, then the disease-free equilibrium $\mathcal{E}^0$ is globally asymptotically stable.*

Proof. Consider the following Lyapunov function:

$$\begin{aligned}\mathcal{V}(t) &= \left(\frac{\beta^\alpha}{(\sigma^\alpha+\mu^\alpha)}+\frac{\beta^\alpha\sigma^\alpha(\mu^\alpha+\theta^\alpha+d^\alpha)}{(\sigma^\alpha+\mu^\alpha)(\mu^\alpha+d^\alpha)(\mu^\alpha+\theta^\alpha+d^\alpha+c^\alpha)}\right)E(t) \\ &\quad+\left(\frac{\beta^\alpha(\mu^\alpha+d^\alpha+\sigma^\alpha\theta^\alpha)}{(\mu^\alpha+d^\alpha)(\mu^\alpha+\theta^\alpha+d^\alpha+c^\alpha)}\right)I(t)+\frac{\beta^\alpha}{(\mu^\alpha+d^\alpha)}L(t).\end{aligned} \tag{15}$$

Then the fractional time derivative of $\mathcal{V}(t)$ along the solutions of model (5) yields :

$$\begin{aligned}{}_b^cD_t^\alpha\mathcal{V}(t) &= \left(\frac{\beta^\alpha}{(\sigma^\alpha+\mu^\alpha)}+\frac{\beta^\alpha\sigma^\alpha(\mu^\alpha+\theta^\alpha+d^\alpha)}{(\sigma^\alpha+\mu^\alpha)(\mu^\alpha+d^\alpha)(\mu^\alpha+\theta^\alpha+d^\alpha+c^\alpha)}\right){}_b^cD_t^\alpha E(t) \\ &\quad+\left(\frac{\beta^\alpha(\mu^\alpha+d^\alpha+\sigma^\alpha\theta^\alpha)}{(\mu^\alpha+d^\alpha)(\mu^\alpha+\theta^\alpha+d^\alpha+c^\alpha)}\right){}_b^cD_t^\alpha I(t)+\frac{\beta^\alpha}{(\mu^\alpha+d^\alpha)}{}_b^cD_t^\alpha L(t).\end{aligned} \tag{16}$$

$$\begin{aligned}&= \beta^\alpha\left[\left(\frac{\beta^\alpha}{(\sigma^\alpha+\mu^\alpha)}+\frac{\beta^\alpha\sigma^\alpha(\mu^\alpha+\theta^\alpha+d^\alpha)}{(\sigma^\alpha+\mu^\alpha)(\mu^\alpha+d^\alpha)(\mu^\alpha+\theta^\alpha+d^\alpha+c^\alpha)}\right)\left(S(t)+\gamma^\alpha H(t)\right)-1\right] \\ &\quad\times\left[E(t)+I(t)+L(t)\right].\end{aligned} \tag{17}$$

Since $S(t)\leq S^0, H(t)\leq H^0, \left(S^0+\gamma^\alpha H^0=\frac{\Lambda^\alpha(\mu^\alpha+\kappa^\alpha+\gamma^\alpha\tau^\alpha)}{\mu^\alpha(\mu^\alpha+\kappa^\alpha+\tau^\alpha)}\right)$ for $t\geq 0$ we have:

$$\begin{aligned}{}_b^cD_t^\alpha\mathcal{V}(t) &\leq \beta^\alpha\left[\left(\frac{\beta^\alpha}{(\sigma^\alpha+\mu^\alpha)}+\frac{\beta^\alpha\sigma^\alpha(\mu^\alpha+\theta^\alpha+d^\alpha)}{(\sigma^\alpha+\mu^\alpha)(\mu^\alpha+d^\alpha)(\mu^\alpha+\theta^\alpha+d^\alpha+c^\alpha)}\right)\left(\frac{\Lambda^\alpha(\mu^\alpha+\kappa^\alpha+\gamma^\alpha\tau^\alpha)}{\mu^\alpha(\mu^\alpha+\kappa^\alpha+\tau^\alpha)}\right)-1\right] \\ &\quad\times\left[E(t)+I(t)+L(t)\right]. \\ &= \beta^\alpha\left[\mathcal{R}_0-1\right]\left[E(t)+I(t)+L(t)\right]\end{aligned} \tag{18}$$

Therefore, ${}_b^cD_t^\alpha\mathcal{V}(t)<0$ holds if $\mathcal{R}_0<1$. Furthermore, ${}_b^cD_t^\alpha\mathcal{V}(t)=0$ if $\mathcal{R}_0=1$. Thus, the largest invariant set of ${}_b^cD_t^\alpha\mathcal{V}(t)$ is a singleton such that $S(t)=S^0$, $H(t)=H^0$, $E(t)=I(t)=L(t)=0$. Therefore, from the LaSalle's invariance principle [33] that the disease-free equilibrium of model (5) denoted by $\mathcal{E}^0$ is globally asymptotically stable whenever $\mathcal{R}_0\leq 1$. This completes the proof. □

Next, we investigate the global stability of the endemic equilibrium point $\mathcal{E}^*$ of model (5) when $\mathcal{R}_0 > 1$.

Theorem 3.2. *If $\mathcal{R}_0 > 1$, then model (5) has a globally asymptotically stable endemic equilibrium point.*

Proof. In order to analyze the global asymptotic stability of the endemic equilibrium of model (5) we set:

$x = \frac{S}{S^*}$, $y = \frac{H}{H^*}$, $z = \frac{E}{E^*}$, $u = \frac{I}{I^*}$, and $v = \frac{L}{L^*}$

Thus, model (5) is transformed into the following form:

$$\left.\begin{aligned}
{}_b^cD_t^\alpha x(t) &= x\left\{\frac{\Lambda^\alpha}{S^*}\left\{\frac{1}{x}-1\right\}-\beta^\alpha E^*(z-1)-\beta^\alpha I^*(u-1)-\beta^\alpha L^*(v-1)\right\}\\
&\quad +x\left\{\frac{\kappa^\alpha H^*}{S^*}\left\{\frac{y}{x}-1\right\}\right\},\\
{}_b^cD_t^\alpha y(t) &= y\left\{\frac{\tau^\alpha S^*}{H^*}\left\{\frac{x}{y}-1\right\}-\gamma^\alpha\beta^\alpha E^*(z-1)-\gamma^\alpha\beta^\alpha I^*(u-1)-\gamma^\alpha\beta^\alpha L^*(v-1)\right\},\\
{}_b^cD_t^\alpha z(t) &= z\left\{\frac{\beta^\alpha S^*I^*}{E^*}\left\{\frac{xu}{z}-1\right\}+\frac{\beta^\alpha\gamma^\alpha H^*I^*}{E^*}\left\{\frac{yu}{z}-1\right\}+\frac{\beta^\alpha S^*L^*}{E^*}\left\{\frac{xv}{z}-1\right\}\right\}\\
&\quad +z\left\{\frac{\gamma^\alpha\beta^\alpha H^*L^*}{E^*}\left\{\frac{yv}{z}-1\right\}+\beta^\alpha S^*\{x-1\}+\beta^\alpha\gamma^\alpha H^*\{y-1\}\right\},\\
{}_b^cD_t^\alpha u(t) &= u\left\{\frac{\sigma^\alpha E^*}{I^*}\left\{\frac{z}{u}-1\right\}\right\},\\
{}_b^cD_t^\alpha v(t) &= v\left\{\frac{\theta^\alpha I^*}{L^*}\left\{\frac{u}{v}-1\right\}\right\}.
\end{aligned}\right\} \tag{19}$$

It can easily be verified that model (19) has a unique endemic equilibrium $\mathcal{E}^*(1,1,1,1,1)$, and that the global stability of $\mathcal{E}^*$ is the same as that of model (5).

Consider the Lyapunov function

$$\mathcal{W} = S^*\Big(x-1-\ln x\Big)+H^*\Big(y-1-\ln y\Big)+E^*\Big(z-1-\ln z\Big)$$

$$+\frac{\beta^\alpha(S^*+\gamma^\alpha H^*)(I^*+L^*)}{\sigma^\alpha E^*}I^*\Big(u-1-\ln u\Big)$$

$$+\frac{\beta^\alpha(S^*+\gamma^\alpha H^*)L^*}{\theta^\alpha I^*}L^*\Big(v-1-\ln v\Big). \tag{20}$$

Differentiating $\mathcal{W}$ with respect to t along solutions of (19) yields:

$$\begin{aligned}
{}_b^cD_t^\alpha\mathcal{W}(t) \;=\;& (x-1)\left\{\Lambda^\alpha\left\{\frac{1}{x}-1\right\}-\beta^\alpha E^*S^*(z-1)-\beta^\alpha I^*S^*(u-1)-\beta^\alpha L^*S^*(v-1)\right\}\\
&+(x-1)\left\{\kappa^\alpha H^*S^*\left\{\frac{y}{x}-1\right\}\right\}\\
&+(y-1)\left\{\tau^\alpha S^*\left\{\frac{x}{y}-1\right\}-\gamma^\alpha\beta^\alpha E^*H^*(z-1)-\gamma^\alpha\beta^\alpha I^*H^*(u-1)-\gamma^\alpha\beta^\alpha L^*H^*(v-1)\right\}\\
&+(z-1)\left\{\beta^\alpha S^*I^*\left\{\frac{xu}{z}-1\right\}+\beta^\alpha\gamma^\alpha H^*I^*\left\{\frac{yu}{z}-1\right\}+\beta^\alpha S^*L^*\left\{\frac{xv}{z}-1\right\}\right\}\\
&+(z-1)\left\{\gamma^\alpha\beta^\alpha H^*L^*\left\{\frac{yv}{z}-1\right\}+\beta^\alpha S^*E^*\{x-1\}+\beta^\alpha\gamma^\alpha H^*E^*\{y-1\}\right\}\\
&+\frac{\beta^\alpha(S^*+\gamma^\alpha H^*)(I^*+L^*)}{\sigma^\alpha E^*}(u-1)\left\{\sigma^\alpha E^*\left\{\frac{z}{u}-1\right\}\right\}\\
&+\frac{\beta^\alpha(S^*+\gamma^\alpha H^*)L^*}{\theta^\alpha I^*}(v-1)\left\{\theta^\alpha I^*\left\{\frac{u}{v}-1\right\}\right\}=F(x,y,z,u,v).
\end{aligned} \tag{21}$$

At endemic point we have the following equations:

$$\begin{cases}
(\mu^\alpha+\tau^\alpha) &= \dfrac{\Lambda^\alpha}{S^*}-\beta^\alpha(E^*+I^*+L^*)+\dfrac{\kappa^\alpha H^*}{S^*}\\
(\mu^\alpha+\kappa^\alpha) &= \dfrac{\tau^\alpha S^*}{H^*}-\gamma^\alpha\theta^\alpha\beta^\alpha(E^*+I^*+L^*),\\
(\mu^\alpha+\sigma^\alpha) &= \beta^\alpha(S^*+\gamma^\alpha H^*)+\beta^\alpha(S^*+\gamma^\alpha H^*)\dfrac{I^*}{E^*}+\beta^\alpha(S^*+\gamma^\alpha H^*)\dfrac{L^*}{E^*},\\
(\mu^\alpha+\theta^\alpha+d^\alpha+c^\alpha) &= \dfrac{\sigma^\alpha E^*}{I^*},\\
(\mu^\alpha+d^\alpha) &= \dfrac{\theta^\alpha I^*}{L^*}.
\end{cases} \tag{22}$$

After some algebraic manipulations and simplifications, we have

$${}_b^cD_t^\alpha\mathcal{W}(t) \;=\; (\mu^\alpha+\beta^\alpha E^*)S^*\left\{2-x-\frac{1}{x}\right\}+\kappa^\alpha H^*\left\{2-\frac{y}{x}-\frac{x}{y}\right\}$$

$$+(\gamma^{\alpha}\beta^{\alpha}E^{*}+\mu^{\alpha})H^{*}\left\{3-\frac{1}{x}-y-\frac{x}{y}\right\}+\beta^{\alpha}I^{*}S^{*}\left\{3-\frac{1}{x}-\frac{z}{u}-\frac{xu}{z}\right\}$$

$$+\beta^{\alpha}S^{*}L^{*}\left\{4-\frac{1}{x}-\frac{z}{u}-\frac{u}{v}-\frac{xv}{z}\right\}+\beta^{\alpha}\gamma^{\alpha}H^{*}I^{*}\left\{4-\frac{1}{x}-\frac{x}{y}-\frac{z}{u}-\frac{yu}{z}\right\}$$

$$+\beta^{\alpha}\gamma^{\alpha}H^{*}L^{*}\left\{5-\frac{1}{x}-\frac{x}{y}-\frac{yv}{z}-\frac{z}{u}-\frac{u}{v}\right\}=F(x,y,z,u,v). \tag{23}$$

□

Since the arithmetic mean is greater or equal to the geometric mean, i.e ${}_{b}^{c}D_{t}^{\alpha}\mathcal{W}(t) = F(x,y,z,u,v) \leq 0$, it can easily be verified that ${}_{b}^{c}D_{t}^{\alpha}\mathcal{W}(t) \leq 0$ provided that $S^{*}, H^{*}, E^{*}, I^{*}, L^{*}$ are positive, where the equality ${}_{b}^{c}D_{t}^{\alpha}\mathcal{W}(t) = 0$ holds only for $x = y = z = u = v = 1$. Therefore ${}_{b}^{c}D_{t}^{\alpha}\mathcal{W}(t) \leq 0$ holds. Then the endemic equilibrium point $\mathcal{E}^{*}$ is globally asymptotically stable if $\mathcal{R}_{0} > 1$ by LaSalle's invariance principle [33].

4 Numerical Simulations and Discussion

In this section, we utilize the MATLAB programming language to numerically solve the model system (5) and assess the behavior of solution for fractional-order derivatives. We perform the fractional Adam-Bashforth-Moulton scheme to simulate the model (5) as illustrated below;
Consider the nonlinear differential equation:

$${}_{b}^{c}D_{t}^{\alpha}\Phi(t) = f(t,\Phi(t)), 0 \leq t \leq T, \tag{24}$$

with the following initial conditions:

$$\Phi^{p}(t) = \Phi_{0}^{p}, \quad p = 0,1,2,...[\alpha]-1 \tag{25}$$

Now, with operating by the fractional integral operator on the equation (24), we can obtain on the solution $\Phi(t)$ by solving the following equation:

$$\Phi(t) = \sum_{p=0}^{|\alpha|-1}\frac{\Phi^{p}}{p!}t^{p} + \frac{1}{\Gamma(\alpha)}\int_{0}^{t}(t-\tau)^{\alpha-1}f(\tau,\Phi(\tau))d\tau \tag{26}$$

Diethelm [37] used the predictor-corrector scheme based on the Adam-Bashforth-Moulton algorithm to solve the equation (24). Setting $h = \frac{T}{N}$, $t_{n} = nh$ and $n = 0,1,2,...,N \in \mathcal{Z}^{+}$.

Therefore we can discretized the equation (24) as follows:

$$\Phi_h(t_{n+1}) = \sum_{p=0}^{|\alpha|-1} \frac{\Phi_0^p}{p!} t_{n+1}^p + \frac{h^\alpha}{\Gamma(\alpha+2)} \sum_{m=0}^{n} a_{m,n+1} f(t_m, \Phi_m) + \frac{h^\alpha}{\Gamma(\alpha+2)} f(t_{n+1}, \Phi_{n+1}^v) \tag{27}$$

where

$$a_{m,n+1} = \begin{cases} n^{\alpha+1} - (n-\alpha)(n+\alpha)^\alpha, & m = 0, \\ (n-m+2)^{\alpha+1} + (n-m)^{\alpha+1} - 2(n-m+1)^{\alpha+1}, & 1 \leq m \leq n, \\ 1, & if \quad m = n+1, \end{cases}$$

and the predicted value $\Phi_h^v(t_{n+1})$ is determined by

$$\Phi_h^v(t_{n+1}) = \sum_{p=0}^{|\alpha|-1} \frac{\Phi_0^p}{p!} t_{n+1}^p + \frac{1}{\Gamma(\alpha)} \sum_{m=0}^{n} b_{m,n+1} f(t_m, \Phi_h(t_m)), \tag{28}$$

with

$$b_{m,n+1} = \frac{h^\alpha}{\alpha}((n+1-m)^\alpha - (n-m)^\alpha. \tag{29}$$

The error estimate is

$$\max_{0 \leq m \leq k} |\Phi(t_m) - \Phi_h(t_m)| = O(h^v), \tag{30}$$

with $k \in \mathbb{N}$ and $v = \min(2, 1+\alpha)$.

4.1 Application of Adam-Bashforth-Moulton Scheme to the proposed model

In this section, we used the Adam-Bashforth-Moulton method to numerically solve the nonlinear fractional-order model (5). In the view to the generalized Adam-Bashforth-Moulton

method, the proposed scheme for the model system (5) has the following form:

$$\left.\begin{aligned}
S(t_{n+1}) &= S^0 + \frac{h^\alpha}{\Gamma(\alpha+2)} f_S\big(t_{n+1}, S^v(t_{n+1}), H^v(t_{n+1}), E^v(t_{n+1}), I^v(t_{n+1}), \\
&\quad L^p(t_{n+1})\big) + \tfrac{h^\alpha}{\Gamma(\alpha+2)} \textstyle\sum_{m=0}^{n} a_{m,n+1} f_S\big(t_m, S(t_m), H(t_m), E(t_m), I(t_m), \\
&\quad L(t_m)\big), \\
H_(t_{n+1}) &= H^0 + \frac{h^\alpha}{\Gamma(\alpha+2)} f_H\big(t_{n+1}, S^v(t_{n+1}), H^v(t_{n+1}), E^v(t_{n+1}), I^v(t_{n+1}), \\
&\quad L(t_m)\big) + \tfrac{h^\alpha}{\Gamma(\alpha+2)} \textstyle\sum_{m=0}^{n} a_{m,n+1} f_H\big(t_m, S(t_m), H(t_m), E(t_m), I(t_m), \\
&\quad L(t_m)\big), \\
E(t_{n+1}) &= E^0 + \frac{h^\alpha}{\Gamma(\alpha+2)} f_E\big(t_{n+1}, S^v(t_{n+1}), H^v(t_{n+1}), E^v(t_{n+1}), I^v(t_{n+1}), \\
&\quad L(t_m)\big) + \tfrac{h^\alpha}{\Gamma(\alpha+2)} \textstyle\sum_{m=0}^{n} a_{m,n+1} f_E\big(t_m, S(t_m), H(t_m), E(t_m), I(t_m), \\
&\quad L(t_m)\big),
\end{aligned}\right\}$$

$$\left.\begin{aligned}
I(t_{n+1}) &= I^0 + \frac{h^\alpha}{\Gamma(\alpha+2)} f_I\big(t_{n+1}, S^v(t_{n+1}), H^v(t_{n+1}), E^v(t_{n+1}), I^v(t_{n+1}), \\
&\quad L(t_m)\big) + \tfrac{h^\alpha}{\Gamma(\alpha+2)} \textstyle\sum_{m=0}^{n} a_{m,n+1} f_I\big(t_m, S(t_m), H(t_m), E(t_m), I(t_m), \\
&\quad (t_m)\big), \\
L(t_{n+1}) &= L^0 + \frac{h^\alpha}{\Gamma(\alpha+2)} f_L\big(t_{n+1}, S^v(t_{n+1}), H^v(t_{n+1}), E^v(t_{n+1}), I^v(t_{n+1}), \\
&\quad L(t_m)\big) + \tfrac{h^\alpha}{\Gamma(\alpha+2)} \textstyle\sum_{m=0}^{n} a_{m,n+1} f_L\big(t_m, S(t_m), H(t_m), E(t_m), I(t_m), \\
&\quad (t_m)\big),
\end{aligned}\right\} \tag{31}$$

where

$$\left.\begin{aligned}
S^v(t_{n+1}) &= S^0 + \frac{1}{\Gamma\alpha} \sum_{m=0}^{n} b_{m,n+1} f_S(t_m, S(t_m), H(t_m), E(t_m), I(t_m), L(t_m), \\
H^v(t_{n+1}) &= H^0 + \frac{1}{\Gamma\alpha} \sum_{m=0}^{n} b_{m,n+1} f_H(t_m, S(t_m), H(t_m), E(t_m), I(t_m), L(t_m), \\
E^v(t_{n+1}) &= E^0 + \frac{1}{\Gamma\alpha} \sum_{m=0}^{n} b_{m,n+1} f_E(t_m, S(t_m), H(t_m), E(t_m), I(t_m), L(t_m), \\
I^v(t_{n+1}) &= I^0 + \frac{1}{\Gamma\alpha} \sum_{m=0}^{n} b_{m,n+1} f_I(t_m, S(t_m), H(t_m), E(t_m), I(t_m), L(t_m), \\
L^v(t_{n+1}) &= L^0 + \frac{1}{\Gamma\alpha} \sum_{m=0}^{n} b_{m,n+1} f_L(t_m, S(t_m), H(t_m), E(t_m), I(t_m), L(t_m).
\end{aligned}\right\} \tag{32}$$

In what follows we have:

$$\left.\begin{array}{rcl} {}_b^cD_t^\alpha S(t) & = & f_S(t_m, S(t_m), H(t_m), E(t_m), I(t_m), L(t_m)), \\ {}_b^cD_t^\alpha H(t) & = & f_H(t_m, S(t_m), H(t_m), E(t_m), I(t_m), L(t_m)), \\ {}_b^cD_t^\alpha E(t) & = & f_E(t_m, S(t_m), H(t_m), E(t_m), I(t_m), L(t_m)), \\ {}_b^cD_t^\alpha I(t) & = & f_I(t_m, S(t_m), H(t_m), E(t_m), I(t_m), L(t_m)), \\ {}_b^cD_t^\alpha L(t) & = & f_L(t_m, S(t_m), H(t_m), E(t_m), I(t_m), L(t_m)), \end{array}\right\} \tag{33}$$

Additionally, the quantities

$$\left.\begin{array}{l} f_S(t_{n+1}, S^v(t_{n+1}), H^v(t_{n+1}), E^v(t_{n+1}), I^v(t_{n+1}), L^v(t_{n+1})), \\ f_H(t_{n+1}, S^v(t_{n+1}), H^v(t_{n+1}), E^v(t_{n+1}), I^v(t_{n+1}), L^v(t_{n+1})), \\ f_E(t_{n+1}, S^v(t_{n+1}), H^v(t_{n+1}), E^v(t_{n+1}), I^v(t_{n+1}), L^v(t_{n+1})), \\ f_I(t_{n+1}, S^v(t_{n+1}), H^v(t_{n+1}), E^v(t_{n+1}), I^v(t_{n+1}), L^v(t_{n+1})), \\ f_L(t_{n+1}, S^v(t_{n+1}), H^v(t_{n+1}), E^v(t_{n+1}), I^v(t_{n+1}), L^v(t_{n+1})), \end{array}\right\} \tag{34}$$

are the derivatives from system (33) at the points t_{n+1}, $n = 1, 2, 3...p$.

4.2 Sensitivity analysis of the reproduction number

In this section we perform the sensitivity analysis and investigate what happens to some dependent variables when either one or more its independent variables are altered. To identify the parameters that are strongly correlated positively or negatively to $\mathcal{R}_0$, we conducted global sensitivity analysis of the model system (5) using partial rank correlated coefficient developed in [35] and the values of the parameters used in the model simulations are in table (1).

Definition 4. *(See, [35]) The normalized sensitivity index of $\mathcal{R}_0$ which depends on differentiably of parameter, ζ is defined as follows:*

$$\Phi_\zeta^{\mathcal{R}_0} = \frac{\partial \mathcal{R}_0}{\partial \zeta} \times \frac{\zeta}{\mathcal{R}_0} \tag{35}$$

The implication of the sensitivity analysis is that the model parameters whose sensitivity index is positive increase the magnitude of $\mathcal{R}_0$ whenever they are increased and those with a negative index decrease the $\mathcal{R}_0$ whenever they are increased. From (35), the value of normalized sensitivity index for each parameter used in the model (5) is summarized in table (2):

Table 1: Parameters and values

Symbol	Definition	Value	Units	Source
Λ	Recruitment rate	11,629,200	$year^{-1}$	[12]
μ	Natural elimination rate	0.25	$year^{-1}$	[12]
κ	Vaccination waning rate	0.4	$year^{-1}$	[12]
γ	Modification factor	0.18	unite-less	[12]
τ	Vaccination rate	0.316	$year^{-1}$	[12]
σ	Incubation rate	3.4	$year^{-1}$	[13]
c	Culling rate	0.15	$year^{-1}$	[12]
d	Disease mortality rate	–	$year^{-1}$	fitted
β	Sheep -to-sheep transmission rate	–	$year^{-1}$	fitted
θ	Rate of progression to chronic state	–	$year^{-1}$	fitted

Table 2: Sensitivity analysis of parameters for the model system (5)

Parameter	Λ	μ	κ	γ	τ	σ	c
Index	+1.0000	-1.0000	+0.2955	+0.2565	-0.2955	-0.4200	−0.4942
Parameter	d	β	θ				
Index	-0.5351	+1.0000	+0.4493				

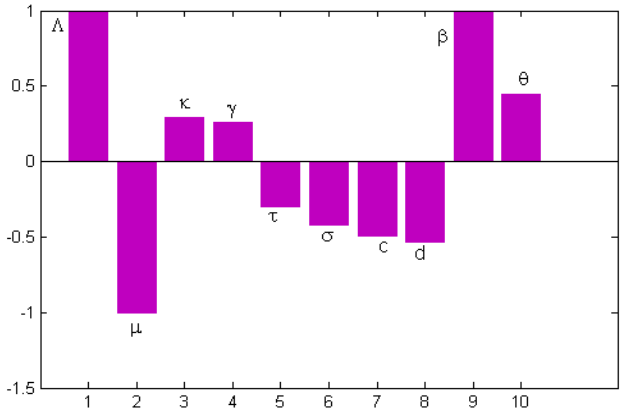

Figure 2: Sensitivity analysis of the model system (5)

From the results in Fig. 2, model parameters with positively partial rank correlation coefficient to $\mathcal{R}_0$, that is., whenever they are increased $\mathcal{R}_0$ increases and those with negatively correlated to $\mathcal{R}_0$, whenever they increased $\mathcal{R}_0$ decreases. Overall, we can note that parameters Λ, κ, γ and θ have high influence on the magnitude of $\mathcal{R}_0$. For example, an increase in Λ by 20% will lead to an increase in the magnitude of $\mathcal{R}_0$ by 20%. On the other-hand, parameters μ, τ, σ, c, and d whenever they increase the magnitude of $\mathcal{R}_0$ decreases. Therefore, to reduce the spread of disease in the population policy markers should target the mitigation that increase the parameters with negative and decrease the parameters with positively correlated to $\mathcal{R}_0$. In particular, we one can note that increasing the vaccination rate (modeled by parameter, τ) and culling rate (modeled by parameter, c) will lead to reduce the spread of disease in the population.

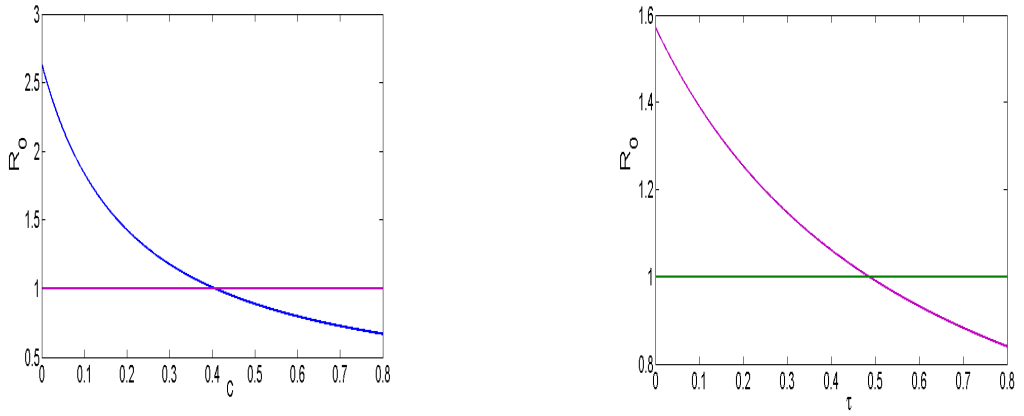

(a) (b)

Figure 3: Effects of varying (a) culling rate c on $\mathcal{R}_0$ (b) vaccination rate τ on $\mathcal{R}_0$

Numerical results in Fig. 3 (a) culling rate (modeled by parameter c) on $\mathcal{R}_0$. From the results we observed that increasing the culling rate on infected sheep decrease the magnitude of $\mathcal{R}_0$. we can note that, whenever c is greater than 0.4 the disease dies in the population. Figure 3 (b), we investigated the effect of vaccination modeled by parameter τ on $\mathcal{R}_0$. We noted that whenever the τ is greater than 0.5 the disease dies in the community.

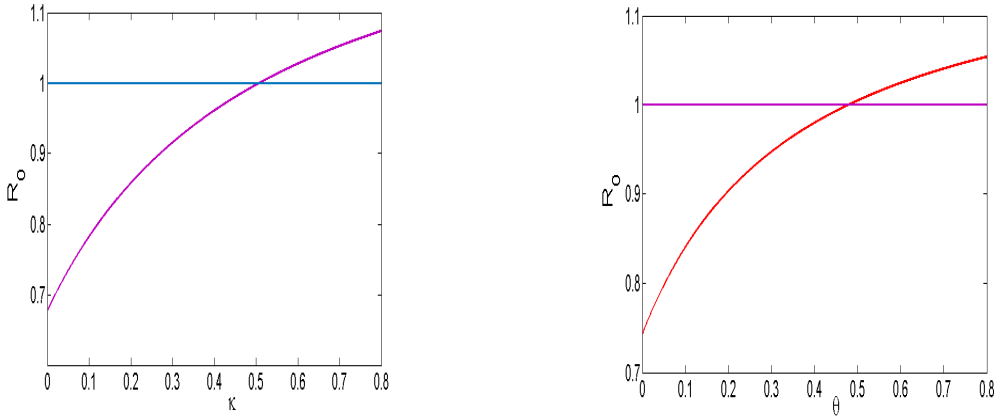

(a) (b)

Figure 4: Effects of varying (a) vaccination waning rate (modeled by parameter κ) on $\mathcal{R}_0$ (b) rate of progression to chronic stage (modeled by parameter θ) on $\mathcal{R}_0$

Numerical results in Fig. 4 (a) we assessed the effects of vaccination waning rate modeled by parameter κ on $\mathcal{R}_0$. From the results we noted that increasing the vaccination waning rate of vaccinated sheep increases the magnitude of $\mathcal{R}_0$. In particular, whenever κ is greater than 0.5 the disease persists in the population. Figure 4 (b), we investigated the effects of rate of progression to chronic stage modeled by parameter θ on $\mathcal{R}_0$. We observed that whenever the θ is greater than 0.5 the disease persists in the community.

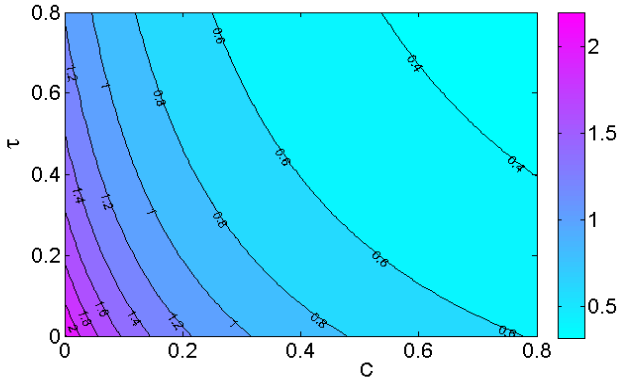

Figure 5: Contour plot of $\mathcal{R}_0$ as the function of culling rate c and vaccination rate τ. We simulated the model (5) at $\theta = 0.015, \quad d = 0.00055,$ and $\quad \beta = 8.444 \times 10^{-6}$

Figure (5) shows the contour plot of $\mathcal{R}_0$ as the function of culling rate c and vaccination rate τ. The results showed that, increase of culling rate on asymptomatic sheep the value of $\mathcal{R}_0$

decreases. In particular, we noted that whenever the culling rate is greater than 0.4 the disease dies out in the population.

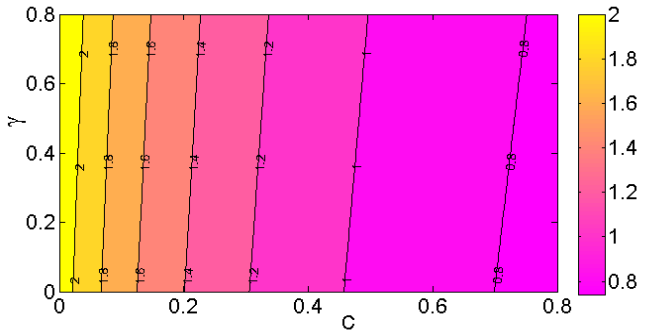

Figure 6: Contour plot of $\mathcal{R}_0$ as the function of culling rate c and modification factor on the disease transmission modeled by parameter γ. We simulated the model (5) at $\theta = 0.015, \quad d = 0.00055, \text{and} \quad \beta = 8.444 \times 10^{-6}$

Figure (5) shows the contour plot of $\mathcal{R}_0$ as the of culling rate c and modification factor on the disease transmission modeled by parameter γ. Overall, we observed that increase of culling rate and modification factor decrease the magnitude of $\mathcal{R}_0$. One can note that whenever the culling rate is greater than 4% the magnitude of $\mathcal{R}_0$ is less than unity.

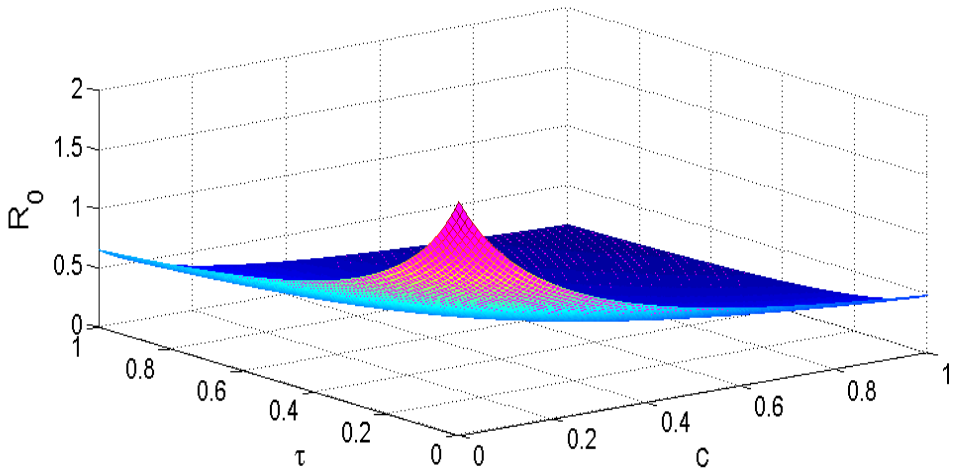

Figure 7: Mesh plot of $\mathcal{R}_0$ as the function of culling rate c and vaccination rate τ. We simulated the model (5) at $\theta = 0.015, \quad d = 0.00055, \text{and} \quad \beta = 8.444 \times 10^{-6}$

Figure (7) shows the mesh plot of $\mathcal{R}_0$ as the function of culling rate (modeled by parameter c) and vaccination rate (modeled by parameter τ). Overall, we noted that increase on culling and vaccination rate decreases the magnitude of $\mathcal{R}_0$. Therefore, we can conclude that both culling and vaccination rate have the potential to minimize the spread of disease in the population.

4.3 Parameter Estimation and model validation using real data

In this section, we utilize the real data of brucellosis cases from Egypt as reported in [34] and estimate the parameters (d, β, θ) that minimize the deviation of real data from prediction of model system (5). Fitting the model using real data and parameter estimation in the fractional order models is an integral part in the disease modeling. Therefore, we utilize both the least squares and Nelder mead algorithm methods [36] to fit and estimate the parameters (d, β, θ) of the model (5). The real data used in this study are yearly reported cases as shown in table (3), and the commutative new infections predicted by the model (5) is obtained using the equation (36):)

$$ {}_{b}^{c}D_{t}^{q}C(t) \quad = \quad \beta^{\alpha}(E(t) + I(t) + L(t))(S(t) + \gamma^{\alpha}H(t)) \tag{36} $$

We use the following function to compute the best fitting:

$$ \mathbb{F} : \mathbb{R}^{3}_{(d,\beta,\theta)} \rightarrow \mathbb{R}_{(d,\beta,\theta)} \tag{37} $$

where d, β, θ are variables such that:

(1) For a given (d, β, θ), we solve the model (5) numerically to obtain a solution $\hat{Y}_i(t) = (\hat{S}, \hat{H}, \hat{E}, \hat{I}, \hat{L}$ which is an approximation of the reported brucellosis cases $Y(t)$.

(2) Set $t_0 = 1$ (the fitting process starts in year 1) and for $t = 2, 3, ..., 13$, corresponding to years in where data are available, evaluate the computed numerical solution for $I(t)$; that is., $\hat{I}(1)$, $\hat{I}(2)$, $\hat{I}(3)$,....., $\hat{I}(13)$.

(3) Compute the root mean square (RMSE) of the difference between $\hat{I}(1), \hat{I}_h(2), ..., \hat{I}(13)$ and real data. This function $\mathbb{F}$ returns the root-mean-square error (RMSE) where

$$ \text{RMSE} = \sqrt{\frac{1}{n}\sum_{k=1}^{13}(I(k) - \hat{I}(k))^2}, \tag{38} $$

(4) Determine a global minimum for the RMSE using Nelder-Mead algorithm. The function $\mathbb{F}$ takes values in $\mathbb{R}^3$ and returns a positive real number.

Using the formula (38), we computed the $RMSE$ that measures the closeness of the model prediction to the real data and was found to be 0.1186. This shows that the proposed model has a good fit to the reported cases. On performing the fitting process we set the following initial conditions $S(0) = 25000$, $H(0) = 10,000$, $E(0) = 100$, $I(0) = 1000$, $L(0) = 20$ and the model parameters are in Table (1).

Table 3: Prevalence of Sheep brucellosis in Egypt from January 1999 through December 2011 based on reports from the General Organization of Veterinary Services in [34]

Year	1999	2000	2001	2002	2003	2004	2005	2006	2007	2008	2009
Cases	1,437	1,303	1,967	1,111	1,755	1,081	1,203	905	924	968	3,095
Year	2010	2011									
Cases	525	292									

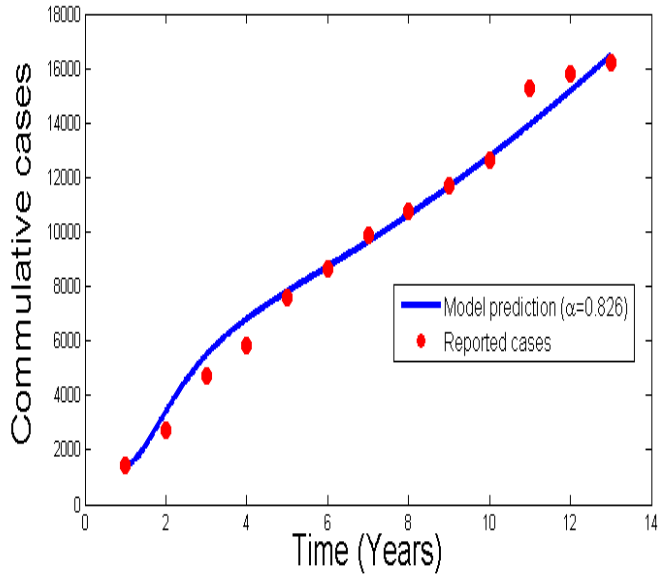

(a)

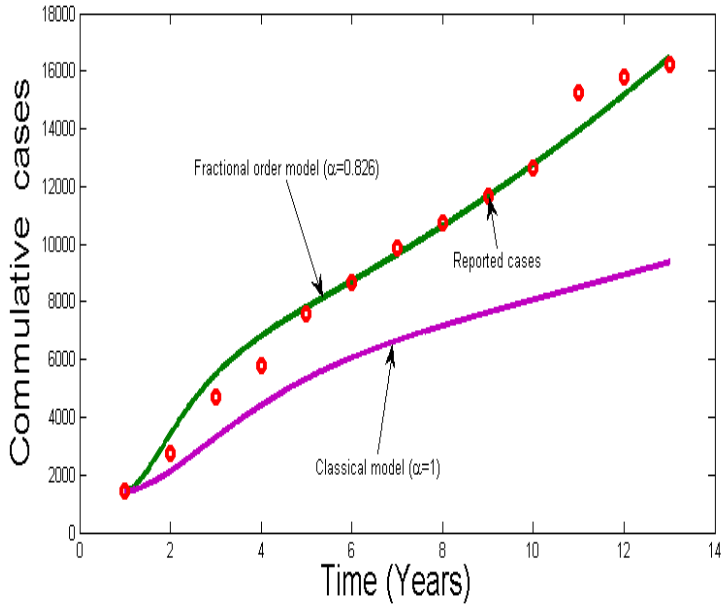

(b)

Figure 8: The model system (5) fitted to brucellosis cases from Egypt as reported in [34] at $\alpha = 0.826$. The *red circles* denote the real data and the *smooth line* denotes the model prediction to the real data.

Figure (8) shows commutative detected cases of brucellosis as reported in Egypt. We used the 13 yearly reports cases to fit in the model system (5). The prediction ability between fractional order model and the classical model is investigated. Overall we observed that the estimates for

the fractional order model are close to the real data for the entire period of 13 years compared to the estimates of the classical integer model. Therefore we conclude that the fractional order model has better forecasts compared to the classical integer model.

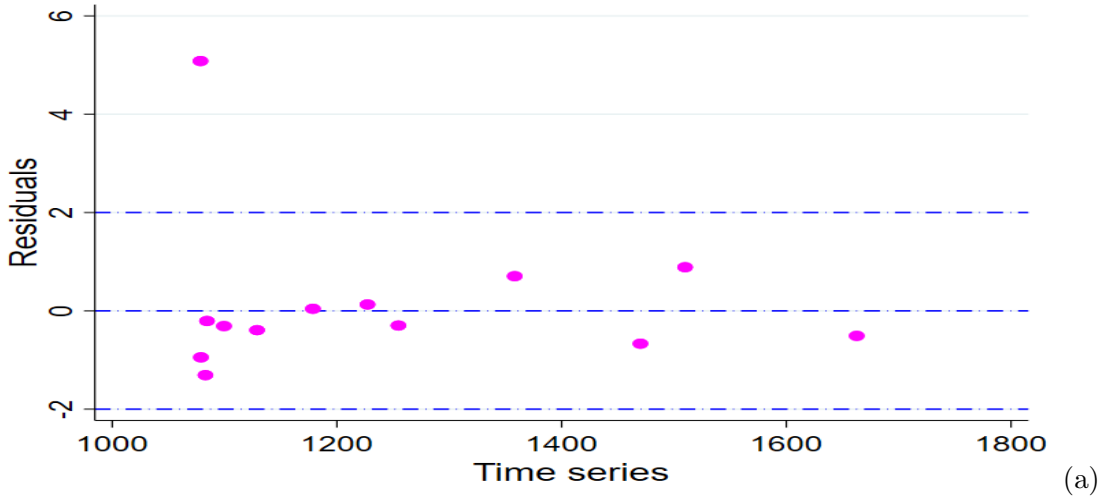

(a)

Figure 9: The model system (5) shows the residuals against the time series for brucellosis cases from Egypt as reported in [34]

Figure (9) shows the graphical representation of residuals for the model system (5) of brucellosis cases reported in [34]. Overall, one can note that the residuals did not follow any particular path (exhibited random pattern) which shows that the model (5) present better forecasts to the reported real data in [34].

4.4 Simulation of the model to support the analytical results

In this section, we solve the model system (5) numerically at $\alpha \in (0, 1]$ to support the analytical results. We first perform the numerical results at $\mathcal{R}_0 < 1$, followed by simulation at $\mathcal{R}_0 > 1$ to show the behavior of dynamical solution of the model (5).

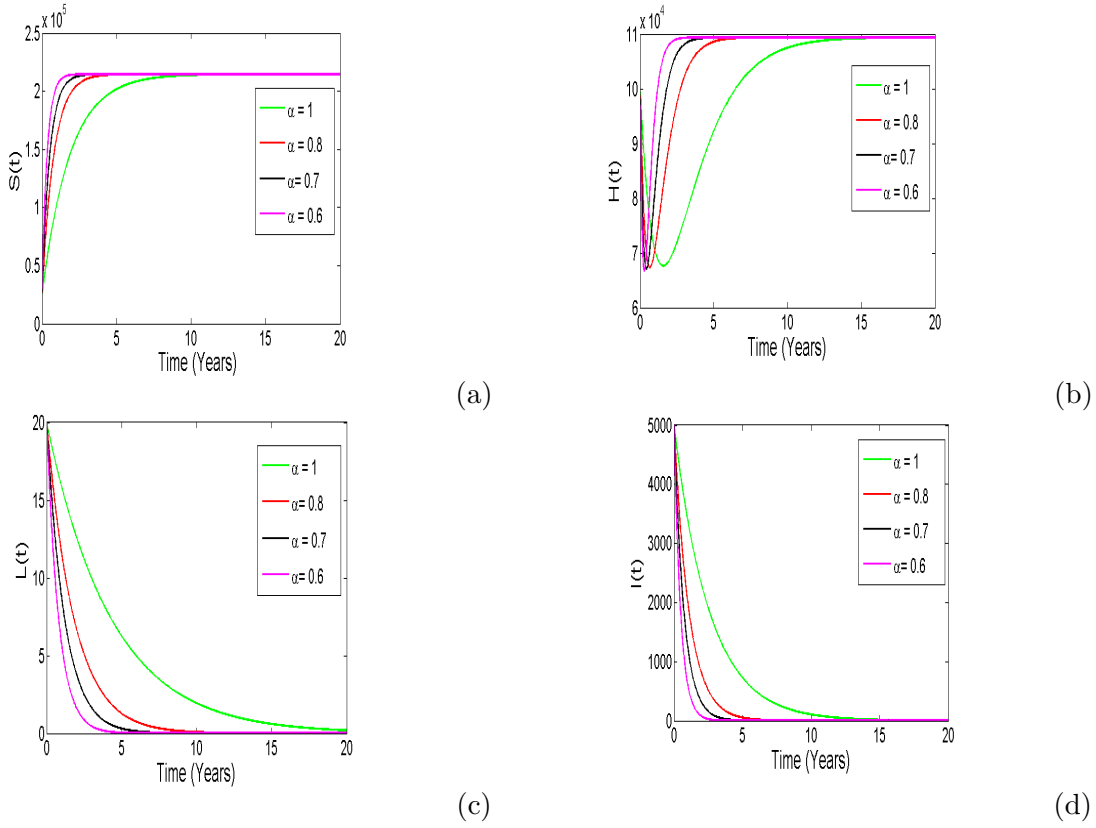

Figure 10: Dynamical solutions of model system (5) at $\mathcal{R}_0 = 0.0142$ with different order derivatives, $\alpha = 0.6,\ 0.7,\ 0.8,\ 1$

Numerical simulation in Fig. (10) shows the convergence of model solutions to the disease-free equilibrium with different fractional order derivatives. The solution were obtained upon setting $d = 1.5 \times 10^{-6}$, $\beta = 8.944 \times 10^{-9}$, and $\theta = 1.5 \times 10^{-5}$, giving $\mathcal{R}_0 = 0.0142$. Overall, we observed that as the order of derivatives decrease from unit the time taken by the solution to converge to the disease-free equilibrium decreases.

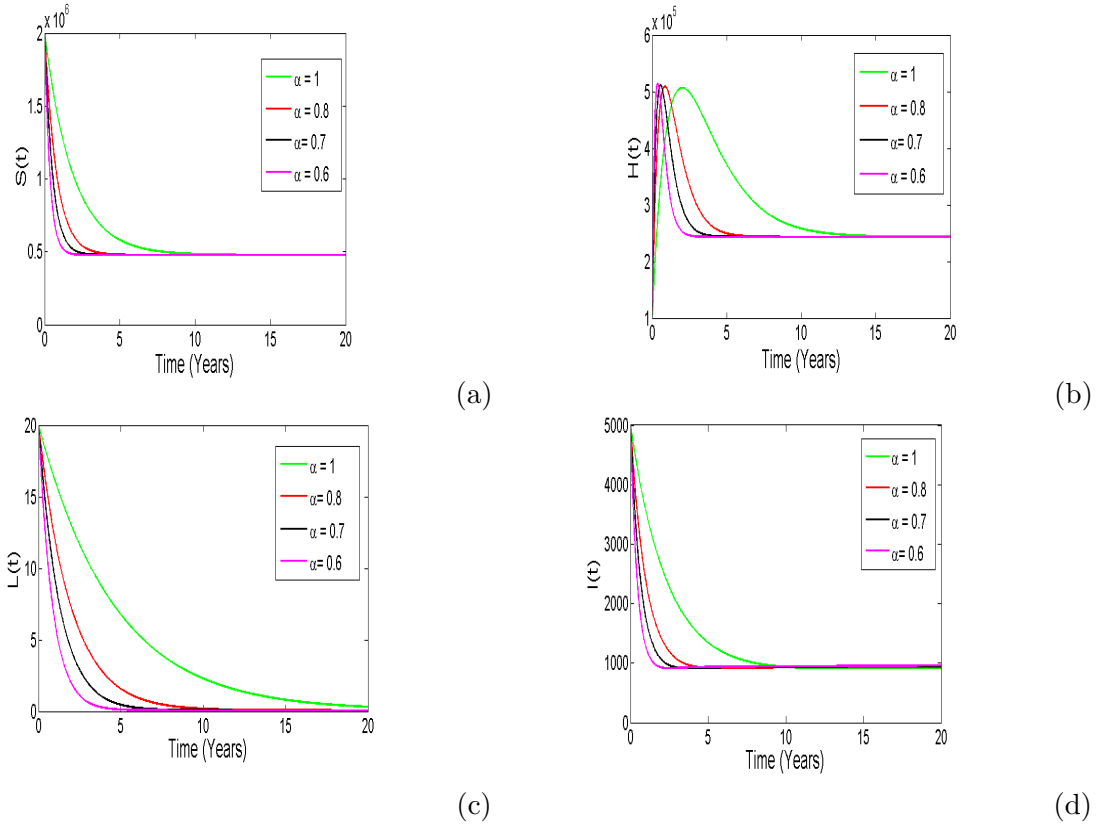

Figure 11: Dynamical solutions of model system (5) at $\mathcal{R}_0 = 9.6235$ with different order derivatives, $\alpha = 0.6,\ 0.7,\ 0.8,\ 1$

Numerical simulation in Fig. (11) shows the convergence of model solutions to the endemic equilibrium with different fractional order derivatives. The solution were obtained upon setting $d = 0.015, \quad \beta = 8.944 \times 10^{-6}$, and $\theta = 1.5 \times 10^{-4}$, giving $\mathcal{R}_0 = 9.6235$. Overall, we observed that whenever the derivative order α approaches 1, the memories of biological species decreases as a result the number of infections increase over time. Additionally, one can note that as the order of derivatives decrease from 1 the time taken by the solution to attain its stability decreases.

5 Concluding Remarks

Brucellosis is one of the zoonotic diseases which is caused by bacteria belong to the genus *Brucella*. This bacteria can cause infections to both wild and domestic animals such as cattle, goats, sheep, dogs, wild hogs and etc. Recently, mathematical modeling of infectious disease

using fractional order derivatives are suggested in the literature [24, 30, 31]. It is worth noting that fractional order models can properly capture the memory effects and hereditary properties of biological systems. Therefore, in this study we analyzed the Caputo derivative non-integer order *Brucellosis* model. We quantitatively studied the model and provided its analysis in details. We investigated the global stability of both disease-free and endemic equilibrium points of non-integer *Brucellosis* model using well constructed Lyapunov functions. We found that the disease free and endemic equilibrium point is global stable whenever $\mathcal{R}_0 < 1$ and $\mathcal{R}_0 > 1$ respectively. In numerical simulations, first of all we qualitatively performed global sensitivity analysis of the model and expressed the relationship between $\mathcal{R}_0$ and the model parameters. Overall, we noted that for the disease management increase in magnitude of the parameters with negative correlation coefficients would significantly reduce the spread of *Brucellosis* disease in the population.

Extensive investigation of the relationship between $\mathcal{R}_0$ and control strategies namely; culling rate (modeled by parameter c) and vaccination rate (modeled by parameter τ) have been investigated. The results revealed that both culling and vaccination rate have the nonlinear relationship with $\mathcal{R}_0$. In particular, we noted that whenever the culling and vaccination rate is greater than 40% and 50% respectively, the disease dies out in the population. Parameter estimation was carried out using the nonlinear least square method which produced best fitted values of d, β and θ. Model validation was carried out using the estimated parameters and the results was compared with both classical integer and fractional order model. Overall, we noted that fractional order model gave better prediction of *Brucellosis* disease compared to integer order derivative. Furthermore, we investigated the role of memory effects on the transmission dynamics of the Brucellosis by varying the order of derivatives α. We observed that the memory of biological species have influence on the dynamics of *Brucellosis* disease transmission. In particular, one can note that as the order of derivatives decrease from 1, the number of infections generated in the population decrease and thus the disease dies in the community.

Availability of Data

All data have been included in the manuscript.

References

[1] Nawal Al Shehhi, Faisal Aziz, Farida Al Hosani, Bashir Aden, and Iain Blair. Human brucellosis in the Emirate of Abu Dhabi, United Arab Emirates, 2010-2015. BMC Infectious Diseases (2016)16:558

[2] Corbel, M.J.; Elberg, S.S.; Cosivi, O. Brucellosis in Humans and Animals;World Health Organization: Geneva, Switzerland; Food and Agriculture Organization of the United Nations: Rome, Italy;World Organization for Animal Health: Paris, France, 2006; ISBN 9241547138.

[3] Blasco, J.M.; Molina-Flores, B. Control and Eradication of Brucella melitensis Infection in Sheep and Goats. Veter.-Clin. North Am. Food Anim. Pr. 2011, 27, 95104.

[4] Aparicio, D.D. Epidemiology of brucellosis in domestic animals caused by Brucella melitensis, Brucella suis and Brucella abortus. Rev. Sci. Tech. lOIE 2013, 32, 5360.

[5] Hasanjani Roush MR, Ebrahimpour S. Human brucellosis: An overview. Caspian J Intern Med 2015; 6(1): 46-47.

[6] Zhang J, Sun G-Q Sun X-D, Hou Q, Li M, et al.(2014). Prediction and control of brucellosis transmission of dairy cattle in Zhejiang Province, China. PloS ONE 9(11):e108592.doi:10.1371/journal.pone.0108592.

[7] Atluri, V.L.; Xavier, M.N.; de Jong, M.F.; den Hartigh, A.B.; Tsolis, R.M. Interactions of the Human Pathogenic Brucella Species with Their Hosts. Annu. Rev. Microbiol. 2011, 65, 523541.

[8] M. Li, G. Sun, G. Sun et al., Transmission dynamics and control for a Brucellosis model in Hinggan League of Inner Mongolia, China, Mathematical Biosciences and Engineering, vol. 11, no. 5, pp. 1115-1137, 2014.

[9] T. Akhvlediani, C. T. Bautista, N. Garuchava et al., Epidemiological and clinical features of Brucellosis in the country of Georgia, PLoS One, vol. 12, no. 1, Article ID e0170376, 2017.

[10] McDermott J, Grace D, Zinsstag J (2013) Economics of brucellosis impact and control in lowincome countries. Rev Sci Tech Off Int Epiz 32: 249-261.

[11] Hou Q and Sun X. Modeling sheep brucellosis transmission with a multi-stage model in Changling County of Jilin Province, China.J.Appl.Math.Comput.DOI 10.1007/s12190-015-0901-y,2015.

[12] Hou Q, Sun X, Zhang, Liu Y, Wang Y, Jin Z. Modeling the transmission dynamics of sheep brucellosis in Innner Mongolia autonomous region, China. Mathematical Biosciences, 242: 51-58, 2013.

[13] Hou Q., Sun X-D. Modeling sheep brucellosis with multi-stage model in Changling Country of Jilin Province, China. J. Appl. math. comput. doi.10.1007/s12190-015-0901-y.

[14] Lou P, Wang L, Zhang X, Xu J, Wang K. Modelling Seasonal Brucellosis Epidemics in Bayingolin Mongol Autonomous Prefecture of Xinjiang, China, 2010-2014. BioMed Research International Volume 2016 (2016), Article ID 5103718, 17 pages http://dx.doi.org/10.1155/2016/5103718

[15] P.O. Lolika, S. Mushayabasa, C.P. Bhunu, C. Modnak, J. Wang Modeling and analyzing the effects of seasonality on brucellosis infection Chaos Solitons Fract, 104 (2017), pp. 338-349.

[16] C. Yang, P.O. Lolika, S. Mushayabasa, J. Wang Modeling the spatiotemporal variations in brucellosis transmission Nonlinear Anal Real World Appl, 38 (2017), pp. 49-67.

[17] Lolika OP, Mohamed Y. A. Bakhet and Ben Saliba Lagure, (2021), Modeling Co-infection of Bovine Brucellosis and Tuberculosis: Asian Research Journal of Mathematics 17(8): 1-13, 2021; Article no. ARJOM.73658 ISSN: 2456-477X, DOI: 10.9734/ARJOM/2021/v17i830319.

[18] Lolika OP and Mushayabasa S, (2021), Dynamics of a Reaction Diffusion Brucellosis Model: Journal of Advances in Mathematics and Computer Science 36(8): 52-69, 2021; Article no. JAMCS.73830, ISSN:2456-9968,DOI:10.9734/JAMCS/2021/v36i830393

[19] Lolika OP, Mushayabasa S (2018). On the role of short-term animal movements on the persistence of brucellosis. Mathematics, 2018, 6, 154.

[20] Olumuyiwa James Peter, "Transmission Dynamics of Fractional Order Brucellosis Model Using CaputoFabrizio Operator", International Journal of Differential Equations, vol. 2020, Article ID 2791380, 11 pages, 2020. https://doi.org/10.1155/2020/2791380.

[21] de Barros, L.C. Lopes, M.M. Santo Pedro, F. Esmi, E. dos Santos, J.P.C. and D.E. Sanchez, "The memory effect on fractional calculus: an application in the spread of COVID-19", *Computational and Applied Mathematics*, 40(3), pp.1-21, 2021.

[22] H.W. Berhe, S. Qureshi, and A.A. Shaikh, "Deterministic modeling of dysentery diarrhea epidemic under fractional Caputo differential operator via real statistical analysis", *Chaos,Solitons & Fractals*, 131, p.109536, 2020.

[23] H. Singh, "Analysis for fractional dynamics of Ebola virus model", *Chaos, Solitons & Fractals*, 138, 109992, 2020.

[24] M. Helikumi, M. Kgosimore, D. Kuznetsov, and S. Mushayabasa, "A fractional-order Trypanosoma brucei rhodesiense model with vector saturation and temperature dependent parameters", Advances in Difference Equations, 1,1-20, (2020).

[25] M. Helikumi, P.O. Lolika "A note on fractional-order model for Cholera disease transmission with control strategies", Commun. Math. Biol. Neurosci. 2022, 2022:30.

[26] Evermann J.F and Eriks I. (1999). Diagnostic mdeicine: the challenges of differentiating infection from disease and making sense for the veterinary clinician. Adv. vet. Sci. com. Med., 41, 25-38.

[27] Grillo M.J., Barberan M. & Blasco J.M. (1997). Transmission of Brucella melitensis from sheep to lambs. Vet. Rec., 140, 602605.

[28] Plommet M., Fensterbak R., Renoux G., Gestin J. & Philippon A. (1973). Brucellose bovine experimentale. Ann. Rech. vt., 4 (3), 419435

[29] Megid J, Luis Antonio Mathias A. L., Robles A. C. Clinical manifestations of brucellosis in domestic animals and humans. The Open Veterinary Science Journal, 2010, 4, 119-126.

[30] Vargas-De-Le'on , "Volterra-type Lyapunov functions for fractional-order epidemic systems", Commun. Nonlinear Sci. Numer.Simul. 24, 7585, 2015.

[31] H. Delavari, D. Baleanu, J. Sadati, "Stability analysis of Caputo fractional-order", Nonlinear systems revisited, Nonlinear Dyn., 67, 2433-2439, 2012.

[32] van den Driessche, P. Watmough, J., "Reproduction number and subthreshold endemic equilibria for compartment models of disease transmission", Math. Biosci., 180, 2948, 2002.

[33] LaSalle, J.S.: The stability of Dynamical Systems. CBMS-NSF Regional Conference Series in Applied Mathematics. vol. 25. SIAM: Philadelphia (1976).

[34] Wareth G., Hila A., Refai M, Melzer F., Roesler U., Neubauer. Animal brucellosis in Egypt. J. Infect Dev Crties, 2014;8(11):1365-1373

[35] Arriola, Leon and Hyman, J, "Forward and adjoint sensitivity analysis with applications in dynamical systems", *Lecture Notes in Linear Algebra and Optimization*, 2005

[36] Nelder J, mead R, "A simplex method for function minimization", *The computer Journal,* Vol. 7, no. 4, pp. 308-313, 1964

[37] Diethelm, Kai, "The analysis of fractional differential equations: An application-oriented exposition using differential operators of Caputo type", *Springer Science & Business Media*, 2020